Research Article

EASL EUROPEAN ASSOCIATION FOR THE STUDY OF THE LIVER | JOURNAL OF HEPATOLOGY

Hepatocellular ballooning in NASH

Stephen Caldwell[1,*], Yoshihiro Ikura[2], Daniela Dias[1,3], Kosuke Isomoto[2], Akito Yabu[2], Christopher Moskaluk[4], Patcharin Pramoonjago[4], Winsor Simmons[1,5], Harriet Scruggs[4], Nicholas Rosenbaum[4], Timothy Wilkinson[6], Patsy Toms[4], Curtis K. Argo[1], Abdullah M.S. Al-Osaimi[1], Jan A. Redick[7]

[1]*GI/Hepatology, University of Virginia, Charlottesville, VA, United States;* [2]*Department of Pathology, Osaka City University, Osaka, Japan;* [3]*Universidade Federal da Bahia, Salvador-Bahia, Brazil;* [4]*Department of Pathology, University of Virginia, Charlottesville, VA, United States;* [5]*Surgical Therapeutic Advancement Center, University of Virginia, Charlottesville, VA, United States;* [6]*Academic Computing Health Sciences, University of Virginia, Charlottesville, VA, United States;* [7]*The Advanced Microscopy Facility, University of Virginia, Charlottesville, VA, United States*

Background & Aims: Hepatocellular ballooning is a key finding in nonalcoholic steatohepatitis (NASH). It is conventionally defined by hemotoxylin and eosin (H&E) staining showing enlarged cells with rarefied cytoplasm and recently by changes in the cytoskeleton. Fat droplets are emerging as important organelles in cell metabolism. To address a possible relation between fat droplets and ballooning, we studied fat staining, H&E, and keratin 18 staining in human NASH.

Methods: Sequential staining and high resolution imaging were used to study freshly prepared cryo-sections from 10 patients with histologically confirmed steatohepatitis using oil red O for fat droplet identification, H&E to identify ballooning, and anti-K18 to confirm cytoskeletal changes. High resolution images were captured at each stage using the Aperio Scanscope. To provide ultrastructural correlation, glutaraldehyde-fixed specimens were studied using transmission electron microscopy (TEM) with serial sectioning for localization of ballooned cells by light microscopy and TEM in identical specimens.

Results: Serial staining consistently demonstrated that hepatocellular ballooning is associated with fat droplet accumulation evident by oil red O positivity and depletion of cytoplasmic keratin 18 with K-18 positive Mallory–Denk bodies (MDB). TEM confirmed the association between osmium stained fat droplets, MDB formation, and cellular enlargement and suggested droplet-associated dilation of the endoplasmic reticulum.

Conclusions: These results indicate a relationship between cellular ballooning, fat droplet accumulation, and cytoskeletal injury in NASH. We speculate that injury to multiple organelles, including fat droplets and endoplasmic reticulum, contribute to this characteristic finding.

Keywords: Cellular ballooning; Steatohepatitis; NASH; NAFLD; Keratin 18; Fat staining; Oil red O.

Received 1 February 2010; received in revised form 25 March 2010; accepted 15 April 2010; available online 25 June 2010

* Corresponding author. Address: GI/Hepatology, Internal Medicine, Box 800708, University of Virginia Health System, Charlottesville, VA 22908-0708, United States. Tel.: +1 434 924 2626; fax: +1 434 924 0491.

E-mail address: shc5c@virginia.edu (S. Caldwell).

Introduction

Hepatocellular ballooning is an important histological parameter in the diagnosis of nonalcoholic steatohepatitis (NASH) [1–3]. It is usually defined, at the light microscopic level, based on hemotoxylin and eosin (H&E) staining, as cellular enlargement 1.5–2 times the normal hepatocyte diameter, with rarefied cytoplasm [4]. In early classification systems of NAFLD, ballooning was a major distinguishing feature of NASH indicating a greater risk of disease progression, which was subsequently confirmed in longitudinal studies [5–7]. Hepatocellular ballooning has also been shown to correlate with fibrosis and to be associated with injury to the cytoskeleton evident as (i) decreased detection of intact cytokeratin 8 and 18, (ii) increased Mallory–Denk bodies, and (iii) increased detection of cytokeratin 18 fragments (M-30) [8–12].

Hepatocellular ballooning is a component of NASH classification schemes and scoring systems including the Brunt criteria and the NAFLD Activity Score (NAS) from Kleiner, although its definition has remained descriptive and subject to significant inter-observer variation [13–15]. Ultrastructural features of ballooning in viral hepatitis have been previously characterized as composed in part of a dilated endoplasmic reticulum sometimes referred to as hydropic change [16,17]. A few ultrastructural studies in NASH have indicated that enlarged cells, often with degenerative changes, contain multiple small fat droplets along with a lesser degree of dilated endoplasmic reticulum in association with Mallory–Denk bodies [18–20]. Immunohistochemical studies have demonstrated that ballooned cells contain oxidized phosphatidylcholine in the phospholipid-rich rim of fat droplets, and show altered expression of fat droplet associated (PAT family) proteins which regulate insulin-sensitive droplet lipase activity [21–23].

To further characterize ballooned cells in NASH, we undertook the current study using oil red O fat staining and standard H&E staining along with anti-cytokeratin 18 IHC in identical

specimens, and high resolution light microscopic digital imaging in NASH patients with varying degrees of histological severity.

Patients and methods

The study subjects consisted of patients with suspected NASH undergoing liver biopsy (Patients 1–3 and 5–10) or autopsy examination (Patient 4). Other diseases were excluded by extensive clinical and laboratory evaluation. The clinical history and standard light microscopy of the biopsy confirmed the diagnosis of NASH in all cases with fibrosis stages ranging from 1 to 4 according to the Brunt classification [13], and a NAS index ranging from 4 to 6 according to Kleiner et al. [14]. Clinical characteristics are summarized in Table 1.

At the time of the biopsy, using a 16 gauge automated coring needle, a separate portion of the biopsy, ranging from 1 to 2 cm, was fixed for at least 2 h in 10% neutral buffered formalin and then mounted for frozen sectioning and subsequent oil red O staining (Polyscientific, Bay Shore, NY) for 3–5 min. Following oil red O staining, and after digital imaging of the fat stained section using the Aperio ScanScope to produce high resolution images (resolution: 0.5 μm per pixel, Aperio ScanScope CS System, Vista, CA), the cover slip was removed in a 15–20 min water rinse followed by conventional H&E staining and subsequent re-imaging of the specimen using the Aperio device. Cover slips were then again removed by the same technique, for anti-keratin 18 immunohistochemical staining in all subjects except for subject 4 which was an autopsy case studied only by H&E and oil red O in serial sections.

Immunohistochemical staining was performed for keratin 18 in the samples which were rehydrated prior to antigen retrieval (Pascal Pressure Chamber with TRS-9 buffer, DAKO, 30 s at 125 °C and 22 psi). Slides were stained using the Dakoautostainer Universal Staining system. Sections were incubated for 10 min with DAKO Dual Endogenous Enzyme Block prior to a 90 min incubation with the primary antibody, CK18 (catalog number 1433-1, Epiomics, dilution 1:40). Sections were subsequently incubated for 45 min with DAKO Envision Dual Link (anti-mouse, rabbit antibody) prior to incubation with chromagen substrate diaminobenzidine tetrahydrochloride (DAB) for 10 min and counterstaining with H&E. Negative controls were performed by omitting the primary antibody. Colon tissue from a normal subject was used as a positive control. In subject 4, a formalin fixed frozen specimen, obtained from a tissue processed less than two hours post mortem, was stained with a 10 min emersion in oil red O, and subsequent conventional photomicroscopy, followed by ethanol rinsing and re-staining with H&E. In all cases, serially stained images were then compared using histological landmarks to assess staining properties of the ballooned cells.

An additional 2 mm portion of the biopsy was obtained for transmission electron microscopy (TEM) from six of the subjects at the time of the biopsy to provide ultrastructural comparison. These specimens were immediately fixed for 2 h in a solution of 4.0% (w/v) paraformaldehyde and 2.0% (w/v) glutaraldehyde in 0.1 M phosphate pH 7.2 buffer at room temperature. The specimens were then post-fixed in 1.0% osmium tetroxide, dehydrated in ethanol, and embedded in resin for sectioning. Semi-thin sections (0.5 μM) were cut from the blocks and stained with toluidine blue for light microscopy. Ultrathin sections (70–80 nm) were cut serially to the semi-thin sections and placed, one section per grid, on 200 mesh copper grids. These were contrast stained with lead citrate and uranyl acetate for examination by TEM. The semi-thin sections stained with toluidine blue were used to identify areas of interest at the light microscopy level to compare to the serially sectioned TEM images.

This research was conducted with approval from the University of Virginia Health Sciences Research Institutional Review Board, and under similar approval from Osaka City University.

Results

As shown in Table 1, all the patients had evidence of active NASH defined, by light microscopy, as steatosis greater than 5%, and varying degrees of inflammatory infiltration and hepatocellular ballooning in the setting of obesity and diabetes and/or hyperlipidemia. In comparisons of H&E, oil red O, and anti-keratin 18 immunohistochemistry stained sections (Figs. 1–3), ballooned hepatocytes evident on H&E staining contained multiple fat droplets and appeared deficient in cytokeratin 18 compared to neighboring cells whether associated with a lower or higher NAS score. Mallory–Denk body formation was also apparent in these cells by H&E and confirmed on anti-keratin 18 staining (Fig. 2). Submembranous staining of anti-K18 reported in some types of ballooning, especially that associated with ischemia–reperfusion by Lackner et al. [11], was not observed. Ultrastructural imaging by TEM revealed characteristic findings of NASH consistent with past studies including cellular enlargement (>30 μm), accumulation of osmiophilic fat droplets, enlarged (longitudinally and spherically) mitochondria with crystalline inclusions and degenerative changes [18,19,24–27]. The latter included areas of dilated endoplasmic reticulum interspersed with and in continuity with the fat droplets as well as Mallory–Denk body formation (Figs. 4 and 5).

Discussion

Cellular ballooning in NAFLD is one of the principle histological findings used to indentify the presence of significant and potentially progressive steatohepatitis. With the exception of keratin 8/18 deficiency, [11] the definition of NASH-related ballooning has remained largely descriptive by H&E staining, and consensus on the underlying pathogenesis has remained elusive. In the present study, we have demonstrated that ballooned hepatocytes in NASH consist substantially of the accumulation of fat droplets evident by the conventional technique of the oil red O stain for

Table 1. Patient characteristics.

Pt	Age	Sex	BMI	Fibrosis Stage (0–4)	NAS (0–8)	Balloon score (0–2)	AST (U/L)	ALT (U/L)	Major risks*	Anti-DM or anti-lipidemia medication**
1	27	F	37.9	2	6	2	64	110	Obesity, DM	Glipizide, sitaglipten
2	65	F	31.9	3	5	1	39	57	Obesity, DM	None
3	32	M	24.5	1	4	1	29	17	Lipidemia	None
4	67	F	29.1	4	6	2	40	37	Over-wt, DM	None
5	71	F	31.8	4	4	2	40	22	Obesity, Lipidemia	Simvastatin
6	43	M	30.1	1	5	1	43	71	Obesity, Lipidemia	None
7	65	M	29.0	2	5	2	45	33	Over-wt, Lipidemia	omega-3 1000 mg/day
8	47	M	31.1	1	5	1	53	115	Obesity, DM	Pioglitazone
9	42	F	48	2	6	2	38	60	Obesity, DM	Metformin, insulin
10	75	F	25.6	1	5	2	154	173	Over-wt, DM	None

* Lipidemia indicates the presence of hyperlipidemia as a risk factor for NASH. DM indicates type 2 diabetes mellitus. Over-wt indicates over-weight.
** Anti-diabetic medications including metformin, incretins, and glitazones or anti-hyperlipidemic medications including statins, fibrates, or omega-3 fatty acid supplements.

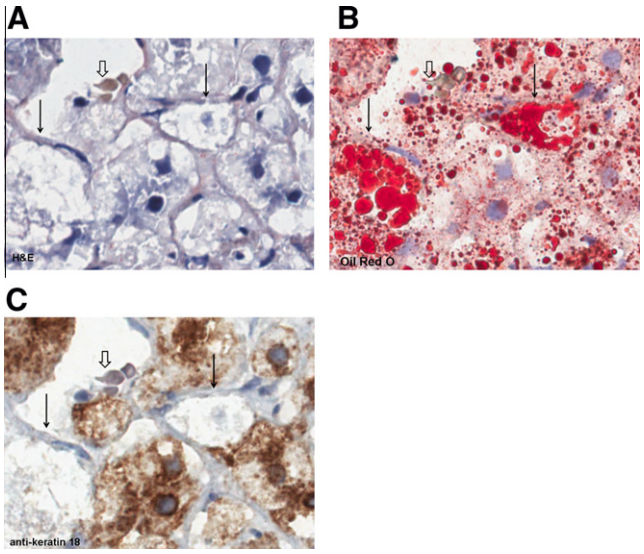

Fig. 1. Patient series 1. (A) H&E, (B) oil red O, (C) anti-K-18. Note oil red O positive droplets and lack of CK-18 staining in two ballooned hepatocytes (solid arrows) compared to anti-K-18 positive neighboring cells. Open arrow indicates landmark red blood cell in central vein. (300× using the Aperio, 0.5 μm per pixel). Indicated magnifications are derived from the scale of the Aperio scanner (0.5 μm per pixel).

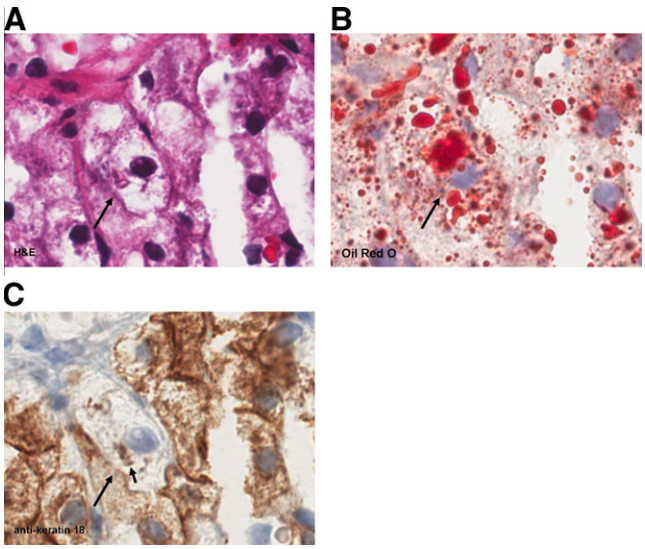

Fig. 2. Patient series 2. (A) H&E, (B) oil red O, (C) anti-K-18. Solid arrow indicates a ballooned hepatocyte which contains (B) numerous oil red O positive fat droplets and (C) show diminished expression of keratin 18 compared to neighboring cells. Note anti-K-18 immunostaining of Mallory–Denk body (arrowhead) in C. (300× using the Aperio, 0.5 μm per pixel). Indicated magnifications are derived from the scale of the Aperio scanner (0.5 μm per pixel).

neutral lipid. These findings support the results of prior studies of hepatocellular ultrastructure in NASH and immunohistochemical studies which demonstrated the presence of oxidized phosphatidylcholine and altered fat droplet associated PAT proteins in the ballooned cells of NASH [21,22].

Although the principle findings of fat droplet accumulation, dilated endoplasmic reticulum, and cytoskeletal injury in ballooned cells could represent independent processes, our results focus additional attention on the potential role of deranged fat

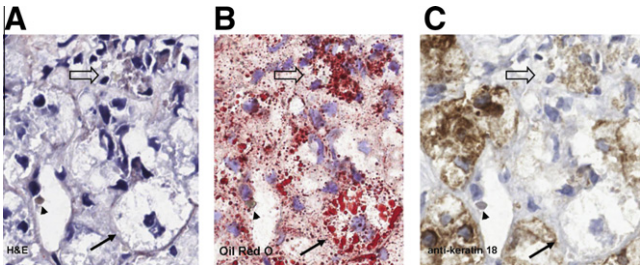

Fig. 3. Patient series 3. (A) H&E, (B) oil red O, (C) anti-K-18. Solid arrow indicates a ballooned hepatocyte. The arrowhead indicates a landmark red blood cell in a central vein. Note the dense fat droplet staining (open arrow) within a necrotic focus suggesting release of these structures with cell death. Indicated magnifications are derived from the scale of the Aperio scanner (0.5 μm per pixel).

droplet metabolism in NASH. Injury to these structures is likely to significantly alter disposal of free fatty acids whose accumulation underlies lipotoxicity. The accumulation of fat droplets in ballooned hepatocytes also suggests involvement of the endoplasmic reticulum from which they are derived and to disturbance in their normal disposal as VLDL particles, impairment of which appears to play a significant role in NASH pathogenesis [28–33]. Because of the close association of ballooning with the formation of Mallory–Denk bodies [34], these results further raise essential questions regarding the interaction of the fat droplets with the cytoskeleton of the hepatocyte. Prior work from Frank et al. demonstrated that adipocyte fat droplets form from the ER in close association with cytoskeletal elements [35,36]. More recent investigation in Drosophila has shown that cytoskeletal associations are maintained in more mature droplets and guide movement of the fat droplets via 'molecular toggles' mediated by members of the PAT family proteins which also govern lipase access to the triglyceride within the fat droplets [37].

The accumulation of fat droplets in ballooned hepatocytes unites several pathogenic mechanisms in NASH including oxidative fat injury, endoplasmic reticulum dysfunction, and abnormalities of the cytoskeleton in hepatocellular ballooning [38–41]. From this work, we can conjecture that oxidative injury to the fat droplet contributes to damage to the endoplasmic reticulum as a result of both fat accumulation and loss of cytoskeleton function. This may obstruct the fat droplet interaction with normal VLDL

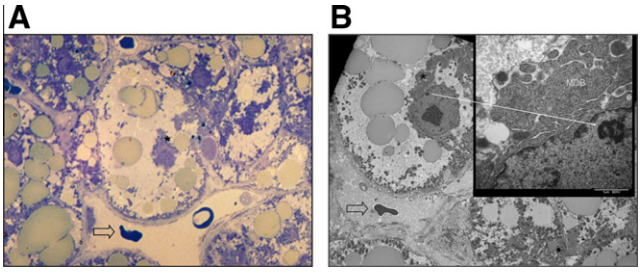

Fig. 4. Serial localization of ballooned cell for correlative light microscopy with toluidine blue and ultrastructure by TEM. (A) Toluidine blue staining of an osmium fixed specimen showing abundance of osmiophilic mediovesicular fat droplets (400×). Open arrow indicates a landmark red blood cell within the central vein. Asterisk indicates Mallory–Denk Body confirmed in the serially cut TEM shown in (B). (B) Serially cut sample to examine by TEM (1000×) the same cell shown in (A). Open arrow indicates landmark red blood cell within the central vein. TEM shows relationships between cellular enlargement, accumulation of fat droplets and Mallory–Denk body (asterisk). Inset (15,000×) confirms the filamentous Mallory–Denk body (MDB). The solid arrow indicates landmark heterochromatin within the nucleus in reference to the inset.

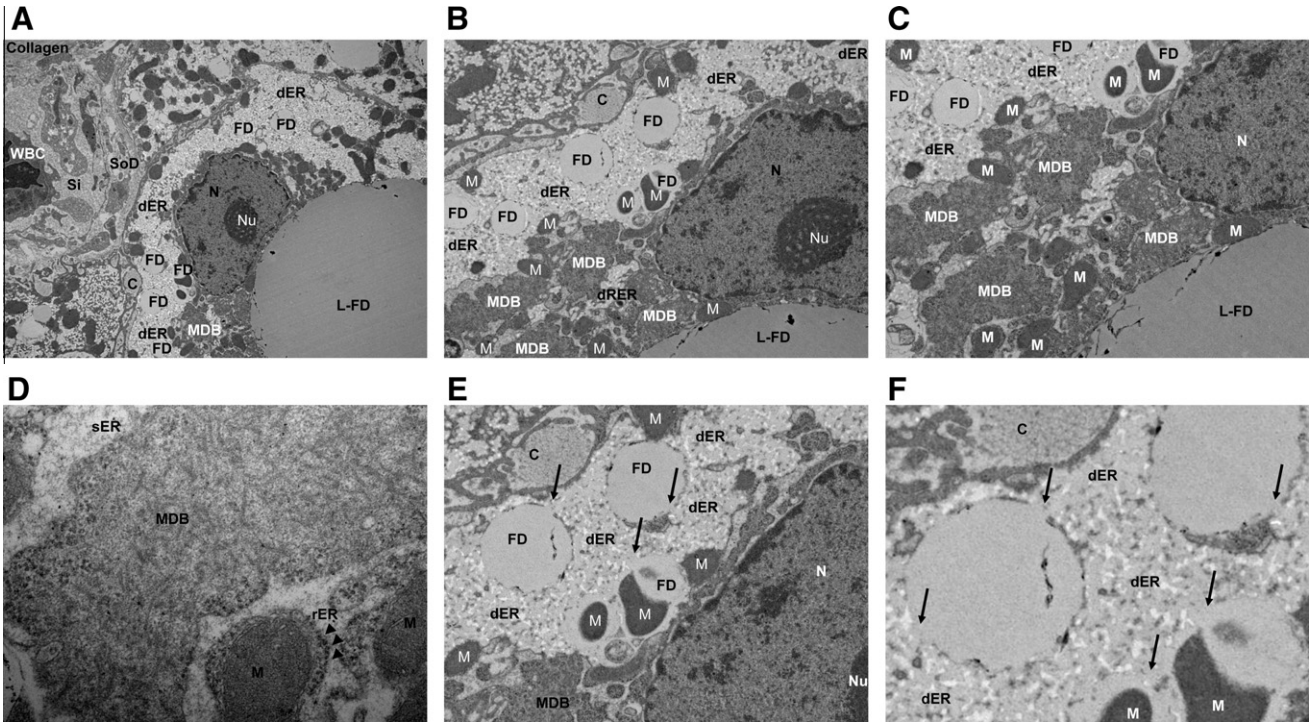

Fig. 5. Representative TEM series. (A–F) Ultrastructure of a ballooned hepatocyte showing the relationships between fat droplets, dilated endoplasmic reticulum, and cytoskeletal injury evident as a perinuclear Mallory–Denk body. (up to 60,000×). *Abbreviations:* L-FD, large fat droplet; FD, fat droplet; Si, sinusoidal space; SoD, space of Disse; C, extracellular collagen bundle; N, nucleus; Nu, nucleolus; M, mitochondria; MDB, Mallory–Denk body; dER, dilated endoplasmic reticulum. (F) Arrows indicate continuity of the fat droplets with the endoplasmic reticulum.

synthesis and secretion and could result in changes in the cytoskeleton evident as a Mallory–Denk body. How this process might interact with abnormal expression, misfolding, hyperphosphorylation, and degradation of keratins 8 and 18, previously described in a number of conditions associated with ballooning and oxidative stress [42], remains to be assessed. Abnormal disposition of the fat droplets in ballooned hepatocytes rather than total fat content might also explain the lack of correlation between the steatosis grade and the degree of ballooning which was recently reported by Chalasani et al. [43].

The authors recognize that this study has inherent limitations. There is often disagreement even among experts about the presence or absence of cellular ballooning in NASH by conventional H&E staining and we anticipate that some readers will disagree with our determination of ballooning in the sample figures we have provided. However, it is our hope that these findings, supported by the consistent results of the keratin 18 stains and serial section cutting of the LM and TEM specimens to localize ballooned cells (Figs. 1–5), will shed light on this difficult area. In addition, while we have studied a relatively wide range of histological severity, the number of subjects is small due to the challenge of prospectively studying human tissue. We also recognize inherent technical limitations of the techniques we used. Although not quantified, penetration of the oil red O fat stain into both ballooned hepatocytes and macrosteatotic cells seemed to vary with dwell time in the stain solution. Because lipid composition is known to affect the activity of this stain [44], lipid composition within the fat droplets may be present and could have altered the appearance of the cells. Indeed, variable composition in hepatic fat droplets has been observed using ion mass spectroscopy on human NAFLD liver biopsy samples and *in vitro* in cell culture using properties of osmium-fat binding [45,46]. Finally, we realize that our study is comparative and only observational but we feel that the findings are valid and offer important insight into the potential role of the fat droplet organelle in this disease. The latter is further supported by recent experimental work indicating an important role of lipophagy of fat droplets in the regulation of lipid metabolism [47].

In summary, our results show that cellular ballooning in NASH is associated with substantial accumulation of fat droplets along with dilation of the endoplasmic reticulum and injury to the cytoskeleton. Although these findings could represent independent processes, it is plausible that the findings unite a number of disparate observations in this disease. We hypothesize that oxidative injury to the fat droplet surface destroys the integrity of this organelle and is related to similar injury to the endoplasmic reticulum evident morphologically as ER dilation and to injury of the cytoskeleton evident as loss of cytokeratin elements and formation of Mallory–Denk bodies. We conjecture that injury to the fat droplet impairs safe disposal of excess free fatty acids and thus contributes to NASH-related cellular lipotoxicity. Whether similar associations are evident in cellular ballooning and cytoskeletal injury in other conditions such as ischemia–reperfusion or cholestatic disease described by both Lackner et al. [11] and by Zatloukal et al. [42] warrants further study.

Conflict of interest

The authors who have taken part in this study declared that they do not have anything to disclose regarding funding or conflict of interest with respect to this manuscript.

Acknowledgements

This study was supported in part by NIH NCCAM Grant 5R21AT2901-2 and in part by a grant to the University of Virginia General Clinical Research Center, 5 M01 RR00847.

References

[1] Yeh MM, Brunt EM. Pathology of nonalcoholic fatty liver disease. Am J Clin Pathol 2007;128:837–847.
[2] Brunt EM. Non-alcoholic steatohepatitis: definition and pathology. Sem Liv Dis 2001;21:3–16.
[3] Contos MJ, Choudhury J, Mills AS, Sanyal AJ. The histological spectrum of nonalcoholic fatty liver disease. Clin Liv Dis 2004;8:481–500.
[4] Brunt EM, Neuschwander-Tetri BA, Oliver D, Wehmeier KR, Bacon BR. Nonalcoholic steatohepatitis: histologic features and clinical correlations with 30 blinded biopsy specimens. Hum Pathol 2004;35:1070–1082.
[5] Matteoni CA, Younossi ZM, Gramlich T, Boparai N, Liu YC, McCullough AJ. Nonalcoholic fatty liver disease: a spectrum of clinical and pathological severity. Gastroenterology 1999;116:1413–1419.
[6] Rafiq N, Bai C, Fang Y, Srishord M, McCullough A, Gramlich T, et al. Long-term follow-up of patients with nonalcoholic fatty liver. Clin Gastroenterol Hepatol 2009;7:234–238.
[7] Ekstedt M, Franzén LE, Mathiesen UL, Thorelius L, Holmqvist M, Bodemar G, et al. Long-term follow-up of patients with NAFLD and elevated liver enzymes. Hepatology 2006;44:865–873.
[8] Gramlich T, Kleiner DE, McCullough AJ, Matteoni CA, Boparai N, Younossi ZM. Pathological features associated with fibrosis in nonalcoholic fatty liver disease. Hum Pathol 2004;35:196–199.
[9] Younossi ZM, Gramlich T, Liu YC, Matteoni C, Petrelli M, Goldblum J, et al. Nonalcoholic fatty liver disease: assessment of variability in pathological interpretations. Mod Pathol 1998;11:560–565.
[10] Zatloukal K, French SW, Stumptner C, Strnad P, Harada M, Toivola DM, et al. From Mallory to Mallory–Denk bodies: What, how and why? Exp Cell Res 2007;313:2033–2049.
[11] Lackner C, Gogg-Kamerer M, Zatloukal K, Stumptner C, Brunt EM, Denk H. Ballooned hepatocytes in steatohepatitis: the value of keratin immunohistochemistry for diagnosis. J Hepatol 2008;48:821–828.
[12] Amidi F, French BA, Chung D, Halsted CH, Medici V, French SW. M-30 and 4HNE are sequestered in different aggresomes in the same hepatocytes. Exp Mol Pathol 2007;83:296–300.
[13] Brunt EM, Janney CG, Di Bisceglie AM, Neuschwander-Tetri BA, Bacon BR. Nonalcoholic steatohepatitis: a proposal for grading and staging the histologic lesions. Am J Gastroenterol 1999;94:2467–2474.
[14] Kleiner DE, Brunt EM, Van Natta ML, Behling C, Contos MJ, Cummings OW, et al. Nonalcoholic steatohepatitis clinical research network. Design and validation of a histologic scoring system for NAFLD. Hepatology 2005;41:1313–1321.
[15] Kleiner DE, Yeh MM, Guy CD, Ferrell L, Cummings O, Contos MJ, et al. Creation of a continuous visual scale of ballooned hepatocytes in nonalcoholic fatty liver disease. Hepatol 2008;48:815A.
[16] Phillips MJ, Poucell S, Patterson J, Valencia P. The liver: an atlas and text of ultrastructural pathology. New York: Raven Press; 1987, p. 45–6.
[17] Lapis K, Schaff Z. Electron microscopy in human medicine. In: Johannessen JV, editor. The Liver, vol. 8. New York: McGraw-Hill; 1979, p. 137–57.
[18] Caldwell SH, Redick JA, Chang CY, Davis CA, Argo CK, Al Osaimi AM. Enlarged hepatocytes in NAFLD examined with osmium fixation: does microsteatosis underlie cellular ballooning in NASH? (Letter). Am J Gastroenterol 2006;101:1677–1678.
[19] Caldwell SH, Redick JA, Davis CA, Brunt EM, Lima VM, Argo CK, et al. Ultrastructural evaluation of hepatocytes with Type 2 Mallory–Denk Bodies: clues to ballooning in nonalcoholic steatohepatitis. Hepatology 2007;46:741A.
[20] Denk H, Stumpter C, Fuchsbichler A, Zatloukal K. Alcoholic and nonalcoholic steatohepatitis: histopathologic and pathogenetic considerations. Pathologe 2001;22:388–398.
[21] Ikura Y, Ohsawa M, Suekane T, Fukushima H, Itabe H, Jomura H, et al. Localization of oxidized phosphatidylcholine in nonalcoholic fatty liver disease: impact on disease progression. Hepatology 2006;43:506–514.
[22] Fujii H, Ikura Y, Arimoto J, Iezzoni JC, Park SH, Itabe H, et al. Perilipin, adipophilin and oxidized phosphatidylcholine in human nonalcoholic steatohepatitis. J Atheroscler Thromb 2009;16:893–901.
[23] Straub BK, Stoeffel P, Heid H, Zimbelmann R, Schirmacher P. Differential pattern of lipid droplet-associated proteins and de novo perilipin expression in hepatocyte steatogenesis. Hepatology 2008;47:1936–1946.
[24] Caldwell S, Swerdlow R, Khan E, Iezzoni J, Hespenheide E, Oelsner D, et al. Mitochondrial abnormalities in NASH. J Hepatol 1999;31:430–434.
[25] Le TH, Caldwell SH, Redick JA, Sheppard BL, Davis CA, Arseneau KO, et al. The zonal distribution of megamitochondria with crystalline inclusions in nonalcoholic steatohepatitis. Hepatology 2004;39:1423–1429.
[26] Caldwell SH, Patrie JT, Brunt EM, Redick JA, Davis CA, Park SH, et al. The effects of 48 weeks of rosiglitazone on hepatocyte mitochondria in human nonalcoholic steatohepatitis. Hepatology 2007;46:1101–1107.
[27] Caldwell SH, Freitas LAR, Park SH, Moreno MLV, Redick JA, Davis CA, et al. Intramitochondrial crystalline inclusions in nonalcoholic steatohepatitis. Hepatology 2009;49:1888–1895.
[28] Fujita K, Nozaki Y, Wada K, Yoneda M, Fujimoto Y, Fujitake M, et al. Dysfunctional very-low-density lipoprotein synthesis and release is a key factor in nonalcoholic steatohepatitis pathogenesis. Hepatology 2009;50:772–780.
[29] Ohsaki Y, Cheng J, Suzuki M, Fujita A, Fujimoto T. Lipid droplets are arrested in the ER membrane by tight binding of lipidated apolipoprotein B-100. J Cell Sci 2008;121:2415–2422.
[30] Tauchi-Sato K, Ozeki S, Houjou T, Taguchi R, Fujimoto T. The surface of lipid droplets is a phospholipid monolayer with a unique fatty acid composition. J Biol Chem 2002;277:44507–44512.
[31] Hermier D, Rousselot-Pailly D, Peresson R, Sellier N. Influence of orotic acid and estrogen on hepatic lipid storage and secretion in the goose susceptible to liver steatosis. Biochem Biophys Acta 1994;1211:97–106.
[32] Cairns SR, Peters TJ. Isolation of micro- and macro-droplet fractions from needle biopsy specimens of human liver and determination of the subcellular distribution of the accumulating liver lipids in alcoholic fatty liver. Clin Sci 1984;67:337–345.
[33] Seki S, Kitada T, Yamada T, Sakaguchi H, Nakatani K, Wakasa K. In situ detection of lipid peroxidation and oxidative DNA damage in non-alcoholic fatty liver diseases. J Hepatol 2002;37:56–62.
[34] Denk H, Stumptner C, Zatloukal K. Mallory bodies revisited. J Hepatol 2000;32:689–702.
[35] Franke WW, Hergt M, Grund C. Rearrangement of the vimentin cytoskeleton during adipose conversion: formation of an intermediate filament cage around lipid globules. Cell 1987;49:131–141.
[36] Schweitzer SC, Evans RM. Vimentin and lipid metabolism. Subcell Biochem 1998;31:437–462.
[37] Welte MA, Cermelli S, Griner J, Viera A, Guo Y, Kim DH, et al. Regulation of lipid-droplet transport by the perilipin homolog LSD2. Curr Biol 2005;15:1266–1275.
[38] Albano E, Mottaran E, Occhino G, Reale E, Vidali M. Role of oxidative stress in the progression of non-alcoholic steatosis. Aliment Pharmacol Ther 2005;22 (Suppl 2):71–73.
[39] Ji C, Kaplowitz N. ER stress: Can the liver cope? J Hepatol 2006;45:321–333.
[40] Puri P, Mirshahi F, Cheung O, Natarajan R, Maher JW, Kellum JM, et al. Activation and dysregulation of the unfolded protein response in nonalcoholic fatty liver disease. Gastroenterology 2008;134:568–576.
[41] Hanada S, Harada M, Kumemura H, Omary MB, Kawaguchi T, Taniguchi E, et al. Keratin-containing inclusions affect cell morphology and distribution of cytosolic cellular components. Exp Cell Res 2005;304:471–482.
[42] Zatloukal K, Stumptner C, Fuchsbichler A, Fickert P, Lackner C, Trauner M, et al. The keratin cytoskeleton in liver diseases. J Pathol 2004;204:367–376.
[43] Chalasani N, Wilson L, Kleiner DE, Cummings OW, Brunt EM, et al. Relationship of steatosis grade and zonal location to histological features of steatohepatitis in adult patients with non-alcoholic fatty liver disease. J Hepatol 2008;48:829–834.
[44] Fowler SD, Greenspan P. Application of Nile red, a fluorescent hydrophobic probe, for the detection of neutral lipid deposits in tissue sections: comparison with Oil red O. J Histochem Cytochem 1985;33:833–836.
[45] Debois D, Bralet M-P, Le Naour F, Brunelle A, Laprevote O. In situ lipidomic analysis of nonalcoholic fatty liver by cluster TOF-SIMS imaging. Anal Chem 2009;81:2823–2831.
[46] Cheng J, Fujita A, Ohsaki Y, Suzuki M, Shinohara Y, Fujimoto T. Quantitative electron microscopy shows uniform incorporation of triglycerides into existing lipid droplets. Histochem Cell Biol 2009;132:281–291.
[47] Singh R, Kaushik S, Wang Y, Xiang Y, Novak I, Komatsu M, et al. Autophagy regulates lipid metabolism. Nature 2009;458:1131–1135.